

Laser-Assisted Bioprinted Skin Equivalent for Cosmetic Efficacy Evaluation

Valérie Andre-Frei¹, Sébastien Cadau¹, Delphine Rival¹, Nicolas Berthelemy¹, Guillaume Fargier¹, Marine Salducci², Delphine Fayol², Fabien Guillemot²

¹ BASF Beauty Care Solutions, 32 rue St Jean de Dieu, 69007 Lyon, France

² Poietis, Bioparc Bordeaux Métropole, 27 Allée Charles Darwin, 33600 Pessac, France

Keywords: Laser-assisted bioprinting, bioprinted skin, 2nd harmonic generation microscopy, ultrastructure, collagen network

This publication was originally presented as a poster presentation at the 24th IFSCC conference in Seoul, South Korea, October 23 - 25, 2017.

INTRODUCTION

Although 3D printing itself is a relatively new technology invented three decades ago, it contributes to one of the most promising medical technological advances of the century in bioscience. The first description of bioprinting appeared in 1988 when R.J. Klebe described cytoscribing, the first 2D and 3D construction of synthetic tissues on fibronectin substrate using an

inkjet printer and computer-assisted high-precision positioning of cells [1]. Since then, significant progress has been made in the development of *in vitro*-bioprinted substitutes that mimic human skin. A 3D printing technology – referred to as bioprinting - is exploited to make cell-loaded scaffolds to produce constructs which better match native tissues. Bioprinting facilitates the simultaneous and highly specific deposition of multiple types of skin cells and biomateri-

als in a short timeframe, a process feature missing in conventional skin tissue-engineering approaches [2]. These bioprinted skin substitutes – also referred to as skin equivalents – contain dermal and epidermal components and offer promising applications either in regenerative medicine as skin grafts or *in vitro* research for the establishment of human skin models to study the safety or efficacy of chemicals or cosmetic ingredients [3-5].

Abstract

Innovative laser-assisted bioprinting and 2nd harmonic generation microscopy methods were combined to produce skin equivalents in less than three weeks and provide advanced 3D-structural and non-invasive information on the fibrillar bioprinted skin networks obtained after treatment with cosmetic ingredients, respectively.

Two different printing technologies were combined to print 3D skin equivalents: a microvalve technology to print collagen layers and laser-assisted bioprinting to deposit cell patterns. A synergistic complex of two peptides (acetyl tetrapeptide 9 & 11) targeting syndecan-1 and

lumican for epidermal and dermal strengthening was supplied during the 18 days of skin printing and maturation. The skin architecture was then analyzed by confocal microscopy associated with a multiphoton laser to generate a 2nd harmonic signal specific to fibrillar collagen and keratin without exogenous staining.

3D-stack image acquisition made it possible to generate a 3D reconstruction of the entire bioprinted skin and reveal particularly the bioprinted skin structure and demonstrated that the peptide complex improves the density and organization of the extracellular collagen fibers in the upper part of the 3D-bioprinted dermis.

Bioprinting is an advanced additive manufacturing platform based on conventional 3D printing that enables the predefined deposition of biomaterials, living cells, and growth medium using computer-aided design (CAD) to fabricate custom-designed tissue constructs by a layer-by-layer printing process with a high degree of flexibility and repeatability [2]. The 3D bioprinting process for human skin tissue is a 3-step manufacturing process consisting of: 1) pre-processing, i.e., tissue design, including cell selection, biomaterials selection and blueprint design of skin tissue; 2) processing, i.e., tissue biofabrication and 3) post-processing, i.e., tissue maturation, including cell proliferation, tissue remodeling and maturation after printing of skin constructs. The functionality, including biochemical and physiologic characterization of the printed skin tissue, is then determined during an additional evaluation step [6].

Depending on the printing modality (bioink deposition mechanism), the representative techniques of cellular bioprinting can be categorized into three types: droplet-based, extrusion-based, and stereolithography (Figure 1). Extrusion-based bioprinting delivers a continuous filament and stereolithography utilizes the spatially controlled irradiation of laser (or light) to solidify a geometrically 2D pattern layered through selective photopolymerization in the bioink reservoir. The other technologies are droplet-based, which means that the printed 3D structure results from the assembly of droplets containing cells or biomaterials. The mechanism of the transient pulse for droplet ejection differs among technologies. In laser-assisted bioprinting (LAB), a near infrared pulse laser source is focused on a cartridge made of a cell-containing bioink film spread on

a glass plate. The laser pulse energy is absorbed by the sacrificial layer and converted into kinetic energy resulting in the generation of a cavitation bubble within the bioink film. This bubble triggers the formation of a liquid jet and eventually cell-laden microdroplets, which are then collected on the culture plate. Using a scanning mirror, a liquid jet can be generated at any XY position to create patterns of cell-laden droplets.

Appropriate printing protocols, cell types, and suitable biomaterials are the three major requirements to produce high quality bioprinted skin tissue with physiological structure in terms of cell density and viability, epidermis and dermis thickness, and global tissue maturation. High cell viability is a direct representation of an adequate bioink and printing performance.

According to the bioprinter performance described in Table 1, the various printing technologies have their own advantages and limitations. Broadly, these methods can be classified as laser-assisted and laser-free. The former have very fine spatial resolutions, very high cell viability maintenance and a broad material viscosity potential use but suffer from a low speed and higher cost, whereas the latter have lower spatial resolutions but are cheaper and faster, particularly the inkjet technology, which prints more than 10,000 droplets/s. However, the choice between Inkjet or extrusion should be made according to the material viscosity, which is a limiting factor for these technologies. To reduce the impact of these limitations, multimodal bioprinters combine at least two printing technologies that are jointly used for the fabrication of the same 3D

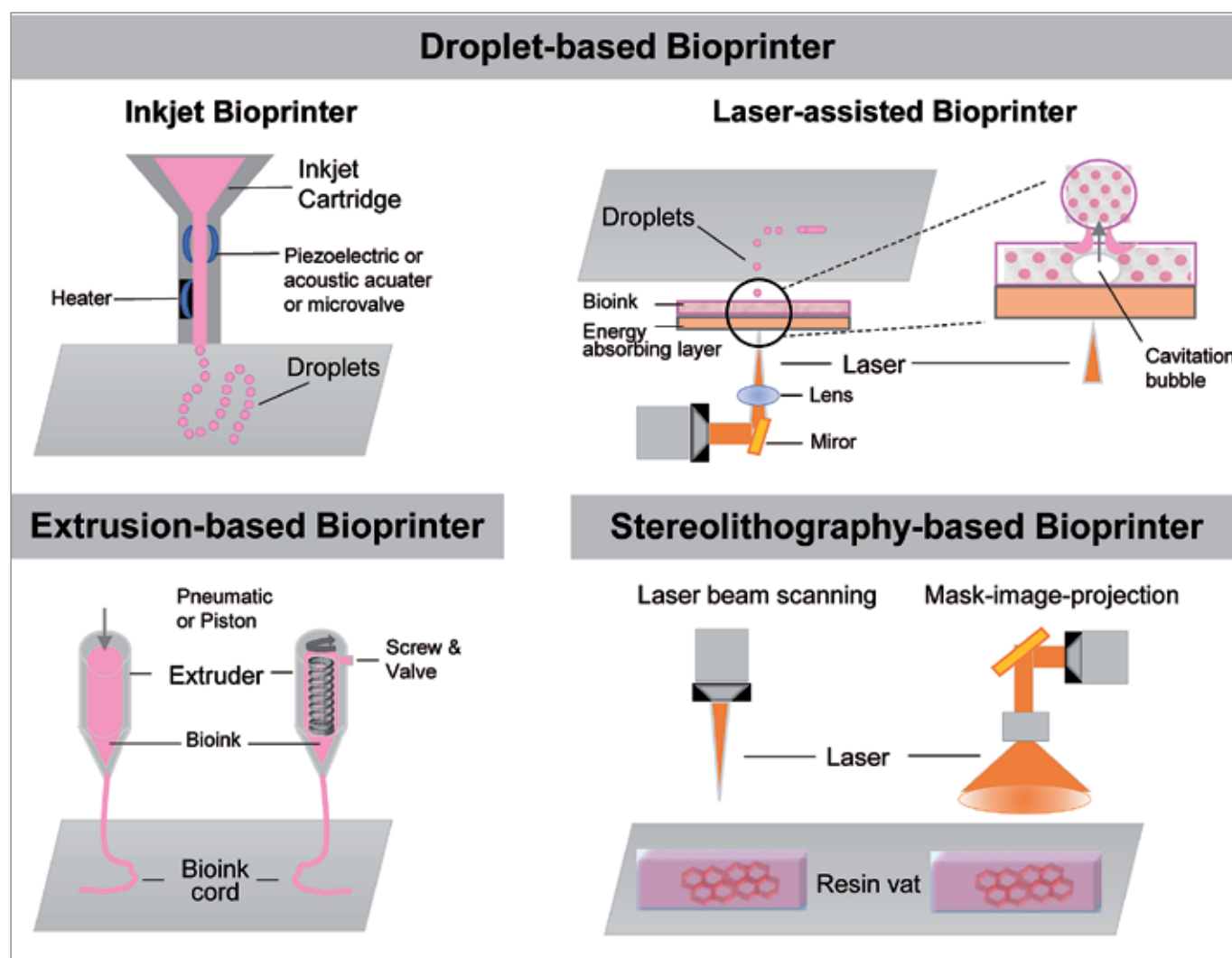


Figure 1 Different technology-based bioprinters, including the specific laser-based bioprinter developed [7-8].

Table I Performance Attributes of Printing Technologies [9-10]

	Inkjet-based	Extrusion-based	Laser-assisted
Resolution/droplet size	50 µm	100 µm	10 µm
Material viscosity/density	Low	High	Medium
Cell viability (post printing)	Medium or high	Medium	High
Single cell control capability	Low	Medium	High
Printing speed (total fabrication time)	Fast	Medium	Medium
Cost	Low	Medium	High

demonstrate the decreases in collagen content and deterioration of organization and functionality occurring with aging [22].

Second-harmonic generation (SHG) is a nonlinear second order optical process combining the advantages of a nonlinear microscopy approach with a coherent modality able to probe molecular organization of fibrillar collagens in normal human skin and 3D reconstructed models without exogenous staining. Interestingly, the structural properties of skin samples analyzed by second harmonic generation

object. Hybridization of technologies enables widening of the working space of the bioprinter performance parameters.

Different printing technologies have been successfully used for skin printing using either sophisticated and complementary inkjet-based, extrusion-based or laser-assisted bioprinters [6]. Recently, it has also been reported that electrohydrodynamic bioprinting can produce constructs with high resolution and throughput [11]. Current skin bioprinting approaches mostly rely on the deposition of fibroblasts and keratinocytes within a homogeneous hydrogel network [6]. Although both naturally-derived (e.g., gelatin, collagen, fibrin, hyaluronic acid, chondroitin sulfate, chitosan, alginate, agarose, dextran, and heparin), synthetic (e.g., polyethylene glycol, polyacrylic acid, polyacrylamide, poly(2-hydroxyethyl methacrylate) or polyvinyl alcohol hydrogels can be utilized for tissue engineering, the natural hydrogels are more appealing due to their high biological affinity, cell signaling properties or their low temperature gelation properties [12]. Some bioprinting skin models are described in **Table II**, including the latest published advanced model containing melanocytes to study the skin pigmentation process and disorders [2, 5, 6, 13-20].

Functionality, including biochemical and physiologic characterization of the printed skin tissue is the final goal for evaluation of cosmetic ingredients. As for conventional, manually produced skin reconstructs, many histological and bio-

Table II Bioprinted Skin Models: Technology, Cells and Bioinks. HFF-1 and NIH-3T3 Fibroblast Cell Lines, Hacat Keratinocyte Cell Line and HNF/HNK/HNM Represent Human Normal Fibroblasts, Keratinocytes and Melanocytes, Respectively.

Technology	Cells	Bioink	Reference
Inkjet	HFF-1 HaCat	Collagen I	Lee et al., 2009 [14]
Laser-Assisted	NIH-3T3 HaCat	Collagen I & Matrigel® layer	Koch et al. 2012 [15]
Micro-extrusion	HNF HNK	Collagen I	Lee et al., 2014 [16]
Micro-extrusion	HNF HNK	Fibrinogen & Alginate & Gelatin	Pourchet et al. 2017 [17]
Laser-Assisted & Inkjet	HNF HNK	Collagen I & Collagen III	Cadau et al., 2017 [5]
Micro-extrusion & Inkjet	HNF HNK	Collagen & polycaprolactone mesh	Kim et al. 2017 [18]
Micro-extrusion & Inkjet	HNF HNK	Skin derived extracellular matrix	Kim et al. 2018 [19]
Inkjet	HNF HNK HNM	Collagen I	Min et al., 2018 [20]

chemical protocols can be applied to evaluate both the bioprinted skin structure and metabolism, with some limitations linked to the biomaterials used. However, no protocol for evaluation of the mechanical properties has been adapted yet from those applied to conventional skin equivalents [21]. Nevertheless, analysis of the bioprinted skin ultrastructure could provide some information regarding the potential functionality of fibrillar networks. In the skin, collagens play a pivotal role for the maintenance of structural integrity and in determining tissue function. Type I collagen is a fibrillar collagen that forms fine, isolated and oriented fibers in the papillary dermis and thicker, crisscrossed fibers in the reticular dermis. Multiphoton laser scanning tomography is a technique that makes it possible to

imaging reveal that the presence of cells induces structural changes due to synthesis and organization in the extracellular matrix affecting in particular collagen in the dermis and the keratinocyte network in the epidermis [22]. Such an innovative 3D imaging method could provide interesting information regarding the performance of cosmetic ingredients in skin fibrillar networks of bioprinted skin.

Therefore, the aim of our study was to produce an improved 3D bioprinted skin for application of a cosmetic treatment during the dermis and epidermis maturation phase and to determine whether SHG without exogenous staining is capable of observing differences between the treated and untreated improved 3D bioprinted skin.

EXPERIMENTAL

3D bioprinted skin production

The Poietis proprietary 2nd generation bioprinter combines laser-assisted bioprinting with the microvalve technology (Figure 2). The former is used to print cells and create features in the size range of 10 to 100µm, while the latter is used to print extracellular matrix components (as collagen) in the size range of 100 to 1000 µm. This allows engineering of 3D objects characterized by both precise details and a large size.

The design step consisted of defining the 3D pattern of cells and materials to be printed based on knowledge of the structure, composition and function of native tissues. The 3D pattern of cells was designed using a dedicated and proprietary CAD software (Figure 2). Parametric studies were conducted to determine the optimal printing parameters given the targeted pattern features. Collagen printing was performed using the microvalve technology. Pressure was used to vary droplet size and hence the deposited vol-

ume. The pattern was chosen to trigger droplet coalescence into a uniform layer, which was then allowed to gel at 37°C before the next fibroblast-containing layer was printed on top of it. Fibroblasts and keratinocytes were printed using the laser-assisted bioprinting technology suppress LAB. The 3D cell pattern was defined by both the XYZ position of the cell-containing droplets and the number of cells per drop. These two parameters can be tuned to vary independently the local cell density and the mean bulk cell density. The number of cells per drop was controlled either by the laser pulse energy or the bioink concentration. The number, thickness and repetition of collagen layers alternating with fibroblast layers was planned to obtain a 200µm thick dermis compartment.

Laser-assisted bioprinted dermis (0.8cm²) was made of alternating multilayers of collagen (bovine collagen 95 % type I and 5 % type III, CellSystems, Troisdorf, Germany, reference 5026-D, 2-3 mg/ml) and primary human fibroblasts (18yo – 60,000/cm²) to produce the bioprinted dermis. Bioprinted

dermis was matured for 5 days in DMEM/F12 medium (Lifetechnologies, Carlsbad, CA, USA) with 10% bovine calf serum (Hyclone, Logan, UT, USA), 100 µg/ml normocine (InvivoGen, San Diego, CA, USA), 5 to 50 µg/ml ascorbic acid (Bayer, Hockenheim, Germany). The number and repetition of collagen layers alternating with fibroblasts layers was adjusted to obtain samples thick enough to be processed for analysis [5]. To produce laser-assisted bioprinted full thickness skin (LaBP FTS), primary human keratinocytes (CELLnTEC, Bern, Switzerland, 3 years old) were printed on top of the dermis (>200,000/cm²), cultured in Green medium (Sigma, St. Louis, MO, USA) for 2-3 days and then elevated at the air-liquid interface for 7 days or up to 14 days depending on the ingredient to be tested. The cultures were maintained at 37°C and 5 % CO₂ in modified Green medium 0.8 % BSA, 0.12 UI/ml insulin (Sigma), 0.4 µg/ml hydrocortisone (Sigma) and 5 to 50 µg/ml ascorbic acid (laroscorbine 1 g/5 ml, Bayer) and antibiotics (Figure 2).

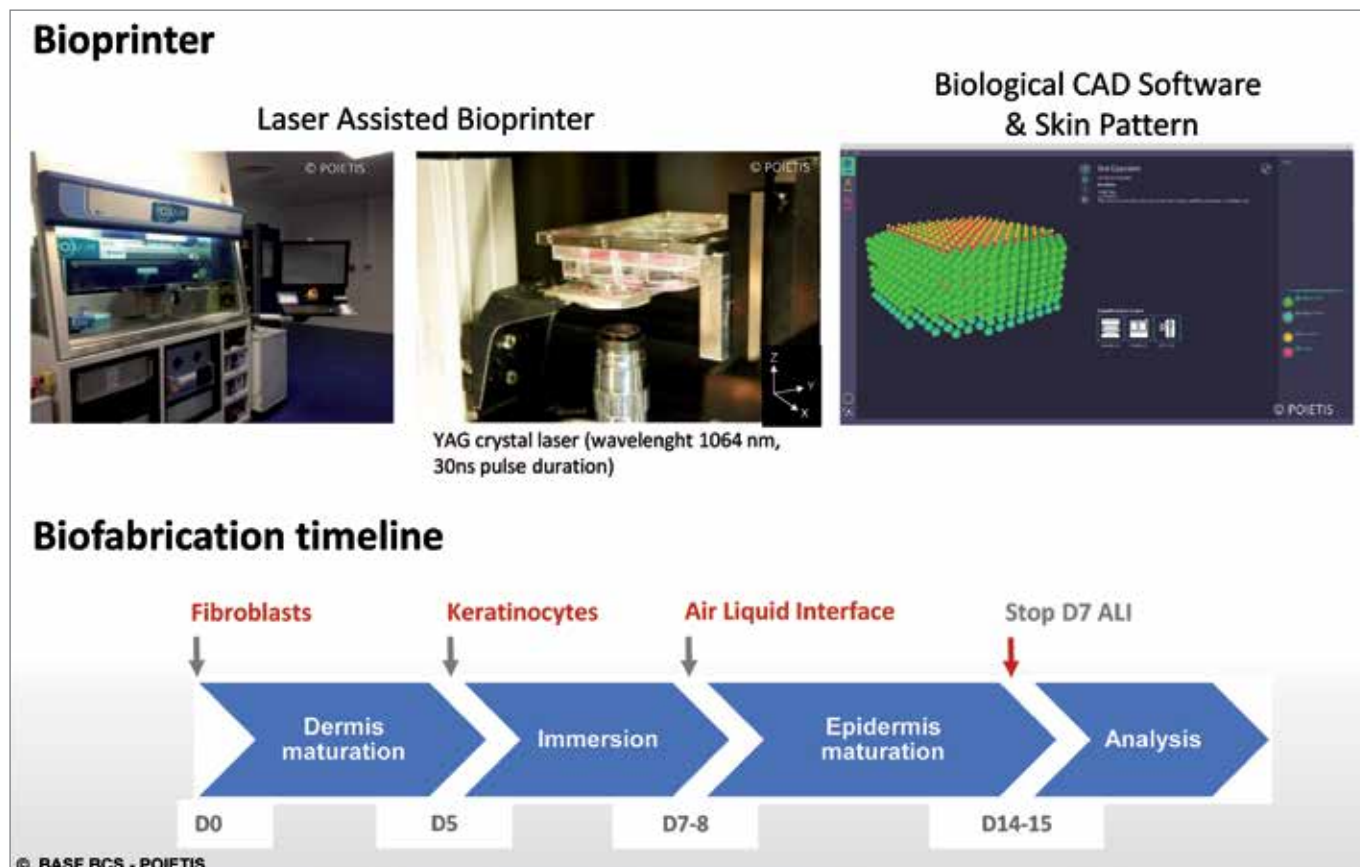


Figure 2 Bioprinting platform and biofabrication timeline.

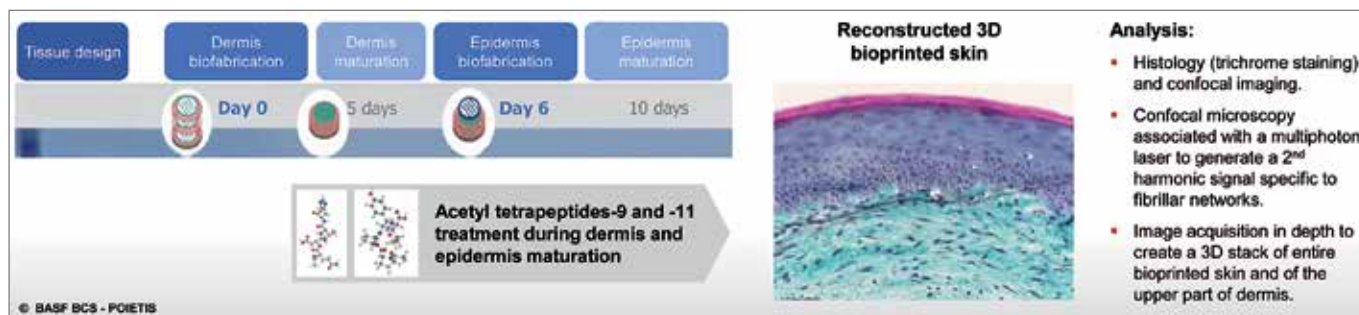


Figure 3 Bioprinted full thickness skin protocol.

Cosmetic treatment and analysis

Treatments with a solution of acetyl tetrapeptide-9 at 7.3 µg/ml and acetyl tetrapeptide-11 at 9.8 µg/ml (BASF BCS, Lyon, France) were administered every two days except when cells were seeded as presented in Figure 3.

Histology

The dermis and epidermis quality was observed by histology (Goldner trichrome) and LaBP FTS, while epidermis and dermis thicknesses were evaluated by image analysis. Cell proliferation and differentiation were evaluated after immunos-

taining of a set of dermal and epidermal markers.

Second harmonic generation (SHG) microscopy

Confocal microscopy (LSM 780, Zeiss, Jena, Germany) associated with a multiphoton laser (Spectra Physics, pulsed laser 800 nm/3300 mW – 400 nm) was used to generate a second harmonic signal specific for the fibrillar skin networks. Acquisition was done with whole bioprinted skin after fixation overnight with paraformaldehyde 4% (Sigma) and without histological cuts. The images were acquired in depth from

the epidermis to dermis to create an entire bioprinted 3D skin image or a 3D stack (10 planes) of the upper part of the dermis. This stack of images was used later for 2D and 3D visualization of the effect of treatment with the active ingredient compared with that of the untreated control condition.

RESULTS AND DISCUSSION

A one-year preliminary trial period was necessary to adjust cell delivery, collagen and cell layer parameters to obtain the most suitable micropattern and the

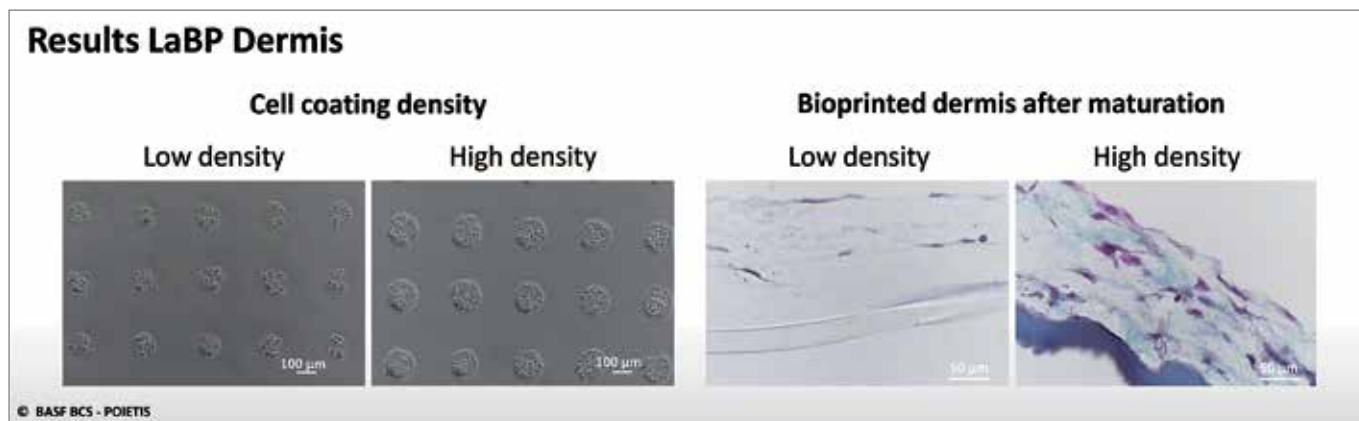


Figure 4 Correlation of fibroblast printing density and quality of laser-assisted bioprinted (LaBP) dermis.

Left: control of fibroblast number delivery/droplet according to printing parameters (cell concentration applied to glass slide and laser parameters), scale bar 100 µm. Right: bioprinted dermis imaging after Goldner trichrome staining, scale bar 50 µm.

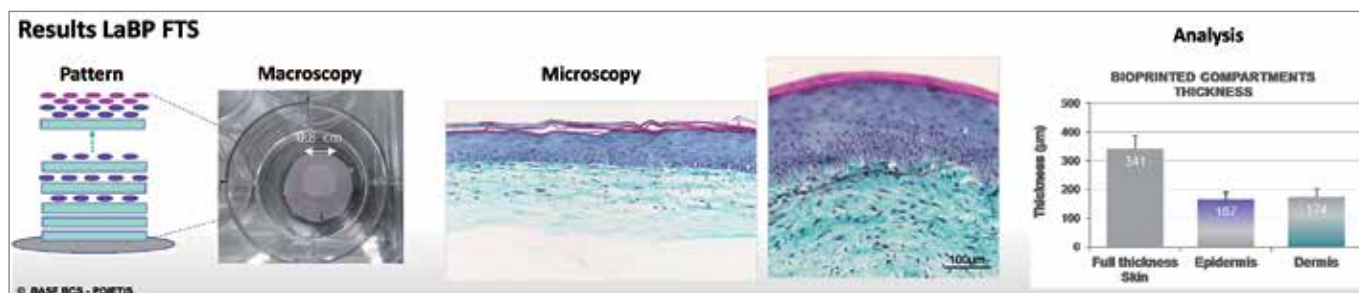


Figure 5 One of the selected printing patterns with examples of the bioprinted skin samples obtained (macroscopy and microscopy – Goldner trichrome staining, scale bar 100 µm) and thickness of the different compartments evaluated by image analysis of 3 samples.

associated protocols to obtain suitable bioprinted skin. The first dermal printing condition selected using a high-density fibroblast printing allowed production of a bioprinted dermis part exhibiting enough fibroblasts in the compartment to sustain fibroblast proliferation and migration to rapidly colonize the bioprinted dermis (**Figure 4**).

However, during dermis maturation and mainly during epidermis maturation, the dermal thickness was dramatically decreased. The printing conditions were adjusted by printing more and thicker collagen layers alternating with denser fibroblast layers. This resulted in an adequate bioprinted skin prototype with a dermal and epidermal thickness, up to 200µm each, suitable for later manipulation and analysis (**Figure 5**).

In this study, the quality of the dermis of bioprinted skin produced in two weeks was demonstrated by a network of numerous entangled neosynthesized collagen fibers revealed by second harmonic

generation (SHG) microscopy. Second harmonic generation is a nonlinear second order optical process combining the advantages of a nonlinear microscopy approach with a coherent modality able to probe the molecular organization of collagens. Using this method, we could easily differentiate the neosynthesized and fibrillar collagen fibers, which appear in grey due to the triple helix structure of long helical domains in tropo-collagen, from the unfolded bioprinted collagen gel (in light gray above the membrane of the culture insert, **Figure 6A**). SHG also makes it possible to clearly differentiate the epidermis from the dermis, as keratinocytes appear in green due to their autofluorescent cytokeratin networks (**Figure 6B**). Regarding the quality of the dermis and epidermis, our bioprinted skin is equivalent to a manually produced one, as we observed a thick dermis containing fibronectin (**Figure 6C**) and a continuous and nicely deposited proliferative basal keratinocyte layer surmounted by regular differentiated keratinocytes (**Figures 6C, 6D**).

To validate this 3D laser-assisted bioprinted skin model, we recently evaluated the effect of a complex of two peptides, acetyl tetrapeptide-9 and acetyl tetrapeptide-11 (7.3 and 9.8 µg/ml, respectively) on the extracellular matrix network (ECM) produced in this model. The complex of two peptides previously selected for its ability to increase the synthesis of lumican, syndecan-1, and collagen types I and XVII in various skin cells (data not shown) visibly improves the organization of the collagen fibers network and structure of the bioprinted dermis part, as evidenced in **Figure 7**. 3D-stack image acquisition makes it possible to generate a 3D-reconstruction of the entire bioprinted skin and to demonstrate particularly that the peptide complex improves the density and organization of the extracellular collagen fibers in the upper part of the 3D-bioprinted dermis (**Figure 7A, 7B**). In the dermis treated with the complex of the two peptides, we observed in its upper part a network of well-defined and very intense collagen fibers (green arrows in **Figure 7D**). In the untreated control

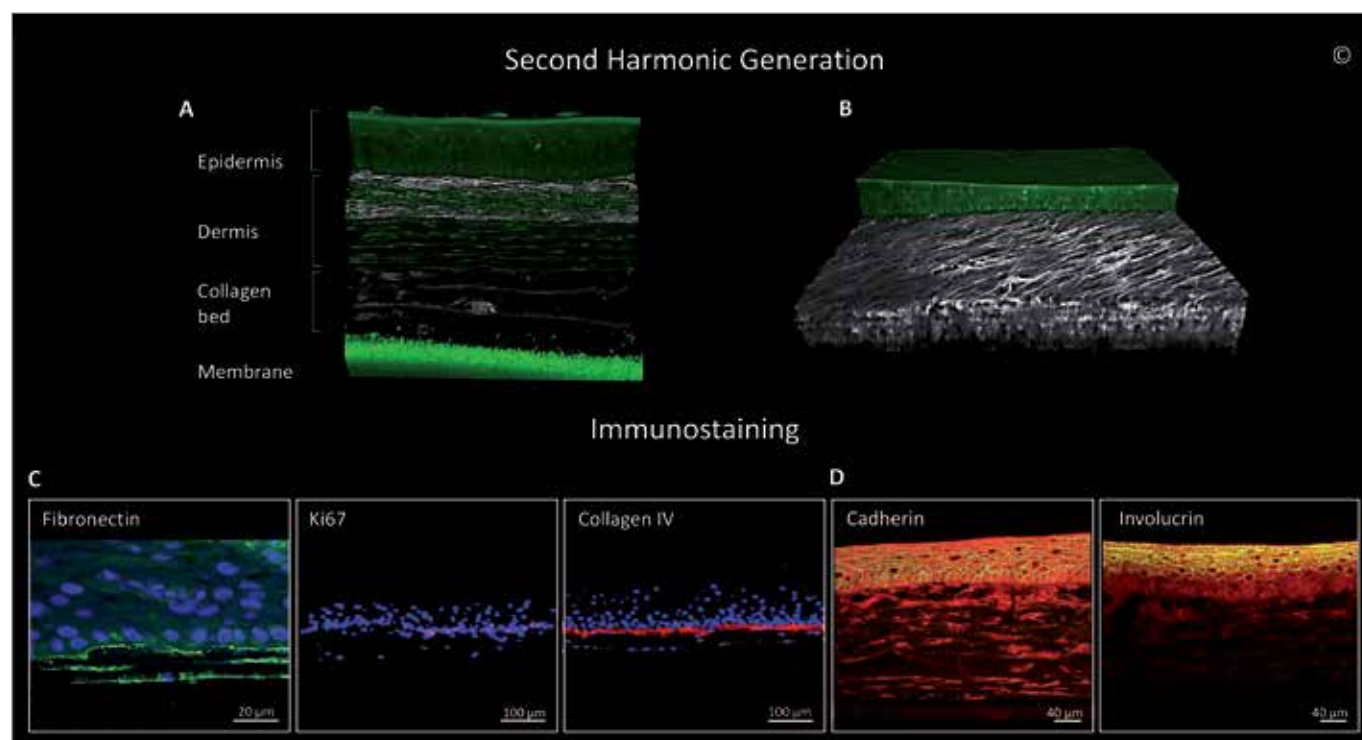


Figure 6 Visualization by second harmonic generation (SHG) microscopy of the fibrillar networks in 3D bioprinted skin. (A) and (B) Fibrillar collagen fibers visualized in grey in the dermis compartment and keratinocytes, fibroblasts and synthetic membrane in green autofluorescence. (C) Visualization by immunostaining of fibroblast synthesis (fibronectin, green), epidermal proliferation (Ki67, red), dermal epidermal junction (collagen IV, red) and nuclei in blue (dapi). (D) Epidermal differentiation evidenced by E-cadherin and involucrin (yellow, counterstaining red).

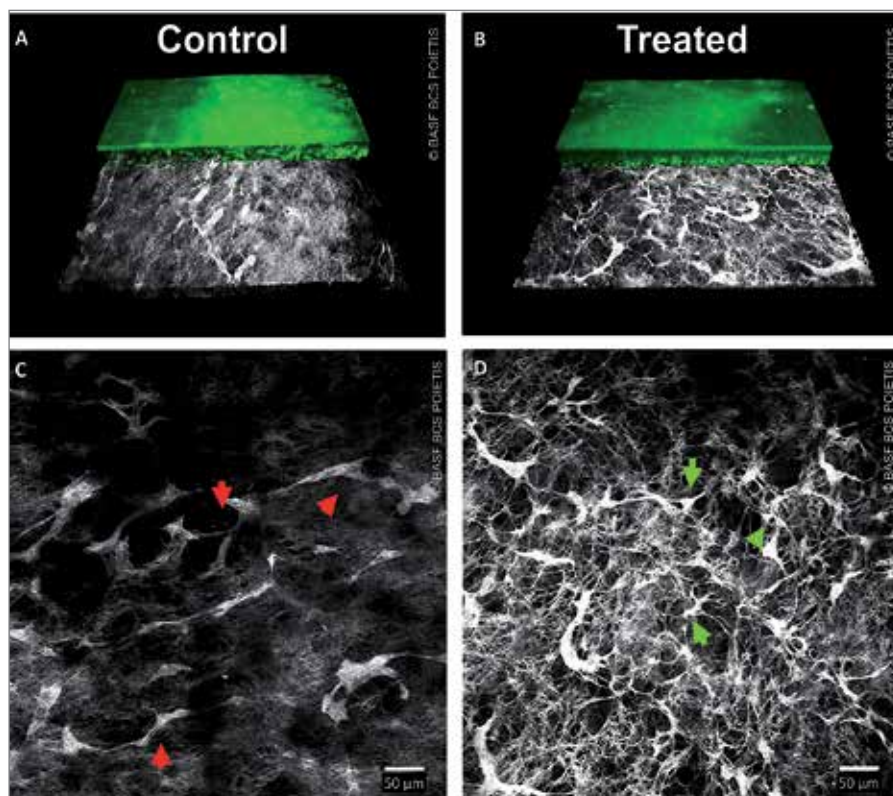


Figure 7 (A) and (B) Visualization by second harmonic generation (SHG) of the effect of treatment with an acetyl tetrapeptide-9/acetyl tetrapeptide-11 complex on the collagenic network in 3D bioprinted skin, (A) control without treatment and (B) treated bioprinted skin. Collagen fibers are visualized in grey, epidermis in green. (C) and (D) Images of a 3D stack acquisition in a depth of 10 planes of the upper part of the dermis, (C) control dermis and (D) treated dermis. Scale bar 50 μm .

condition the fibers are smaller and not as well defined, with a blurry network (red arrows in **Figure 7 C**).

CONCLUSION

Laser-assisted bioprinted skin equivalents are an efficient tool to evaluate the efficacy of cosmetic ingredients. In this study, we particularly improved the quality of the bioprinted skin produced with this innovative method relative to that of our first generation skin, which lacked dermal thickness, although it was suitable for testing cosmetic ingredients [5]. We could show that the laser-assisted bioprinted skin model produced in only 2 weeks instead of the 6 weeks required by the conventional method is equivalent to that of the conventional method in terms of ultrastructure.

We particularly demonstrated that fibroblasts have an excellent cell viability after

printing, as would be expected when using laser assisted bioprinting. Moreover, they could migrate and colonize the bioprinted dermis as well as produce abundant and organized collagenic material, as evidenced by the numerous neosynthesized collagen fibers observed using the innovative 3D second harmonic generation (SHG) microscopic method.

The new protocol makes it possible to obtain in 2 to 3 weeks bioprinted skin constructs that are at least 200 μm and up to 400 μm thick. Moreover, the improved bioprinted skin model was suitable for evaluating the efficacy of an active ingredient within 2 weeks. In addition, we could demonstrate the ability of a peptide complex to improve both the density and the organization of the extracellular collagen fibers in the dermis of 3D bioprinted skin models, providing the dermocosmetic benefit of denser and firmer skin.

References

- [1] Klebe R.J., Cytoscribing: a method for micropositioning cells and the construction of two- and three-dimensional synthetic tissues, *Exp. Cell Res.*, **179**(2) (1988) 362-373.
- [2] Augustine R., Skin bioprinting: a novel approach for creating artificial skin from synthetic and natural building blocks, *Prog. Biomater.*, **7** (2018) 77-92.
- [3] Tarassoli S.P., Jessop Z.M., Al-Sabah A., Gao N., Whitaker S., Doak S. and Whitaker I.S., Skin tissue engineering using 3D bioprinting: An evolving research field, *J. Plast. Reconstr. Aesthet. Surg.*, **71**(5) (2018) 615-623.
- [4] van Kogelenberg S., Yue Z., Dinoro J.N., Baker C.S. and Wallace G.G., Three-Dimensional Printing and Cell Therapy for Wound Repair, *Adv. Wound Care* **7**(5) (2018) 145-155.
- [5] Cadau S., Rival D., Andre-Frei V., Chavan M., Fayol D., Salducci M., Brisson B. and Guillemot F., New bioprinted skin, cosmetic *in vitro* model, *J. Cosmet. Sci.*, **68**(1) (2017) 85-90.
- [6] Yan W.C., Davoodi P., Vijayavenkataraman S., Tian Y., Ng W.C., Fuh J.Y.H., Robinson K.S. and Wang C.H., 3D bioprinting of skin tissue: From pre-processing to final product evaluation, *Adv. Drug Deliv. Rev.* (2018), <https://doi.org/10.1016/j.addr.2018.07.016>.
- [7] Guillemot, F., Laser printing method, and device for implementing said method, F.R. Patent No. 3,030,360 B1- Université de Bordeaux Institut national de la santé et de la recherche médicale (2018).
- [8] Cui H., Nowicki M., Fisher J.P., and Zhang L.J., 3D Bioprinting for Organ Regeneration, *Adv. Healthcare Mater.* **6** (2017) 1601118, <https://onlinelibrary.wiley.com/doi/full/10.1002/adhm.201601118>.
- [9] Derakhshanfar S., Mbeleck R., Xu K., Zhang X., Zhong W. and Xing M., 3D bioprinting for biomedical devices and tissue engineering: A review of recent trends

- and advances. *Bioact. Mater.*, **3**(2) (2018) 144-156.
- [10] *Liu F., Liu C., Chen Q.H., Ao Q., Tian X., Fan J., Tong H. and Wang X.*, Progress in organ 3D bioprinting, *Int. J. Bioprint.*, **4**(1) (2018) 128.
- [11] *Vijayavenkataraman S., Lu W.F. and Fuh J.Y.H.*, 3D bioprinting of skin: a state-of-the-art review on modelling, materials, and processes, *Biofabrication*, **8**(3) (2016), <https://doi.org/10.1088/1758-5090/8/3/032001>.
- [12] *Li Y., Rodrigues J. and Tomas H.*, Injectable and biodegradable hydrogels: gelation, biodegradation and biomedical applications, *Chem. Soc. Rev.*, **41** (2012) 2193-2221.
- [13] *Dos Santos M., Auxenfans C., Thepot A. and Marquete C.*, Utilisation de la bio-impression 3D pour la conception de modèles de peau reconstruite *in vitro*. In: *Cosmetic Valley Editions. Modèles pour l'évaluation des produits cosmétiques : de la molécule à l'humain. 1er volume. Chartres : Grillon Catherine & Marek Haftek; 2018.*
- [14] *Lee W., Debasitis J.C., Lee V.K., Lee J.H., Fischer K., Edminster K., Park J.K. and Yoo S.S.*, Multi-layered culture of human skin fibroblasts and keratinocytes through three-dimensional freeform fabrication, *Biomaterials*, **8** (2009) 1587-1595.
- [15] *Koch L., Deiwick A., Schlie S., Michael S., Gruene M., Coger V., Zychlinski D., Schambach A., Reimers K., Vogt P.M., and Chichkov B.*, Skin tissue generation by laser cell printing, *Biotechnol. Bioeng.*, **109**(7) (2012) 1855-1863.
- [16] *Lee V., Singh G., Trasatti J.P., Bjornsson C., Xu X., Tran T.N., Yoo S.S., Dai G. and Karande P.*, Design and fabrication of human skin by three-dimensional bioprinting, *Tissue Eng Part C Methods*, **20**(6) (2014) 473-484.
- [17] *Pourchet L.J., Thepot A., Albouy M., Courtial E.J., Boher A., Blum L.J., and Marquette C.A.*, Human Skin 3D Bioprinting Using Scaffold-Free Approach. *Adv. Healthc. Mater.*, **6**(4) (2017), <https://onlinelibrary.wiley.com/doi/abs/10.1002/adhm.201601101>.
- [18] *Kim B.S., Lee J.S., Gao G. and Cho D.W.*, Direct 3D cell-printing of human skin with functional transwell system, *Biofabrication*, **9**(2) (2017) 025034.
- [19] *Kim B.S., Kwon Y.W., Kong J.S., Park G.T., Gao G., Han W., Kim M.B., Lee H., Kim J.H. and Cho D.W.*, 3D cell printing of *in vitro* stabilized skin model and *in vivo* pre-vascularized skin patch using tissue-specific extracellular matrix bioink: A step towards advanced skin tissue engineering, *Biomaterials*, **168** (2018) 38-53.
- [20] *Min D., Lee W., Bae I.H., Lee T.R., Croce P. and Yoo S.S.*, Bioprinting of biomimetic skin containing melanocytes, *Exp. Dermatol.*, **27**(5) (2018) 453-459.
- [21] *Tupin S., Molimard J., Cenizo V., Hoc T., Sohm B. and Zahouani H.*, Multiscale Approach to Characterize Mechanical Properties of Tissue Engineered Skin. *Ann. Biomed. Eng.*, **44**(9) (2016) 2851-2862.
- [22] *Koehler M.L., König K., Elsner P., Bückle R. and Kaatz M.*, *In vivo* assessment of human skin aging by multiphoton laser scanning tomography, *Opt. Lett.*, **31** (2006) 2879-2881.

Corresponding Author

Valérie Andre-Frei
 BASF Beauty care Solutions
 Lyon
 France
valerie.andre-frei@basf.com

